The Astrophysical Journal, 605:156–167, 2004 April 10

10 MICRON IMAGING OF SEYFERT GALAXIES FROM THE 12 MICRON SAMPLE

V. Gorjian and M. W. Werner
MS 169-327, Jet Propulsion Laboratory, California Institute of Technology, 4800 Oak Grove Drive, Pasadena, CA 91109; varoujan.gorjian@jpl.nasa.gov, michael.w.werner@jpl.nasa.gov

T. H. Jarrett
Infrared Processing and Analysis Center, Jet Propulsion Laboratory, California Institute of Technology, MS 100-22, Pasadena, CA 91125; jarrett@ipac.caltech.edu

and

D. M. Cole and M. E. Ressler
MS 169-327, Jet Propulsion Laboratory, California Institute of Technology, 4800 Oak Grove Drive, Pasadena, CA 91109; david.m.cole@jpl.nasa.gov, michael.e.ressler@jpl.nasa.gov
Received 2001 December 28; accepted 2003 December 4

ABSTRACT

We present small-aperture (1.″5) photometry and new high-resolution images at 10 μm (N band) for 87 Seyfert galaxies from the Extended 12 μm Sample drawn from the *IRAS* database. With this data we hope to test the predictions of the unified model for active galactic nuclei and to search for bright, extended circumnuclear 10 μm emission. We detected 62 Seyfert galaxies, 18 of which have no previously published small-aperture photometry. All the detected sources, both Seyfert 1's and Seyfert 2's, show a central point source. The 31 Seyfert 1's and 31 Seyfert 2's that we detected have similar luminosity distributions. Except for previously known bright extended 10 μm structure around Arp 220, NGC 1068, and NGC 7469, we see definitive evidence for bright extended emission around only one new object: Mrk 1239. Four other Seyfert 1's and six other Seyfert 2's show evidence of faint, low-level extended emission. One Seyfert 1 and two Seyfert 2's show evidence of significantly increased flux over previously published small-aperture values. We also compared the N-band data with the $J-K_s$ color that we derived from the Two Micron All Sky Survey (2MASS). There is a distinct trend of redder central bulge $J-K_s$ colors corresponding to brighter absolute N-band magnitudes. In color-magnitude space there is a definite grouping of Seyfert 1's and Seyfert 2's, with two sets of outliers.

Subject headings: galaxies: active — galaxies: nuclei — galaxies: Seyfert — infrared: galaxies

1. INTRODUCTION

Seyfert galaxies are the nearest examples of the active galactic nucleus (AGN) phenomenon; hence, by studying them, we increase our understanding of the entire AGN phenomenon from quasars to LINERS. Seyferts fall mainly into two spectroscopically defined types: Seyfert 1's have velocity-broadened wings on their permitted hydrogen lines, while Seyfert 2's lack these broad features. The expectation under the unified model is that the two types are powered by the same inherent mechanism—a black hole with an accretion disk—and that the spectroscopic differences arise simply from differing viewing angles. The model suggests that Seyfert 1's are viewed along the axis of an obscuring dust and gas torus, permitting a direct, unobscured view of the broad-line region (BLR) near the black hole. In contrast, the BLR is blocked from direct view in visible wavelengths by the obscuring torus in Seyfert 2 galaxies (for reviews see Antonucci 1993; Peterson 1997).

The wavelength bands that have been used most often to try to verify the unified model have been the optical and the near-IR. Both have drawbacks for studying emission from the centers of galaxies. Optical nuclear emission can be hard to separate from the optical bulge emission, and optical emission may be heavily attenuated by dust in a host galaxy. While near-IR emission suffers less attenuation by dust, it is still very difficult to separate the nuclear emission from the stellar bulge emission. In contrast, the 10 μm (N-band) window is an excellent spectral region for studying AGNs because stars have relatively little emission at 10 μm and hence 10 μm observations permit good separation of stellar bulge light from non-stellar nuclear light. Moreover, like near-IR, 10 μm radiation is relatively little affected by absorption in the host galaxy.

Previous studies of Seyferts at 10 μm have advanced the field greatly, e.g., Maiolino et al. (1995) and Giuricin, Mardirossian, & Mezzetti (1995); however, the majority of them were performed with bolometers with apertures of 5″–8″ from which no structural or morphological information was gained. Only recently has the availability of mid-IR detector arrays allowed for the high-resolution imaging of AGNs (Bock et al. 2000; Soifer et al. 2000; Krabbe, Böker, & Maiolino 2001). We used the JPL mid-infrared camera (MIRLIN; Ressler et al. 1994) on the Palomar 5 m telescope to image a large sample of AGNs with subarcsecond resolution. These images not only give us better small-aperture photometry; they also allow us to look for structure within the emitting regions of the chosen Seyferts.

We have compiled a large, uniform, imaging sample of Seyferts at 10 μm, from which we hope to address two primary issues. First, we want to test the predictions of the unified model by seeing whether the two Seyfert types look more similar at 10 μm than at shorter wavelengths. Second, we want to search for extended circumnuclear 10 μm emission.

2. THE SAMPLE

To conduct our survey we chose the Seyferts identified in the Extended 12 μm Sample compiled by Rush, Malkan, &

Spinoglio (1993). The 12 μm sample consists of 893 galaxies detected by *IRAS* whose fluxes at 12 μm are greater than 220 mJy and that have Galactic latitude $|b| \geq 25^\circ$. Of these 893 galaxies, 118 are identified as Seyferts by Rush et al. (1993) on the basis of their optical spectra; of those, 95 are accessible at the latitude of Palomar observatory. These 95 galaxies include Seyferts of all types spanning a wide range in luminosity.

Because the *IRAS* beam was large ($45'' \times 4.'5$), the fluxes in the catalog are a combination of the galaxy and AGN fluxes. Many, but not all, of these Seyferts have been observed at 10 μm with smaller apertures. Our survey provides uniform small-aperture photometry for all detected Seyferts.

3. OBSERVATIONS

At 10 μm, the beam size of the 5 m telescope is $0''.5$ (FWHM), while the plate scale of MIRLIN's 128×128 array is $0''.15$ pixel^{-1}, giving an oversampled image over a field of view of $19'' \times 19''$. We had nine clear nights of observing, which allowed us to detect 62 of 87 observed galaxies using the broadband *N* filter ($\lambda_0 = 10.8$ μm, FWHM 5.66 μm).

The MIRLIN observations were taken using the standard chop/nod method of imaging in the mid-IR. The secondary mirror was typically chopped $7''$–$9''$, with similar values for the telescope nod. Two different chopping methods were used in the data accumulation. Initially we used a quad-chop method where the chop and nod were within the $19''$ MIRLIN field of view and the nod and chop directions were perpendicular. After appropriately adding and subtracting the chopped and nodded images, the result was a square pattern of two positive and two negative images. These were then shifted and added to make the final image.

We later switched to a three-beam method where the nod and chop directions were parallel and equal so that, after subtraction, the positive images overlapped, producing a negative image on each side of the positive image. The positive image then had twice as many counts as each negative. During this phase we used a tip/tilt secondary for better image quality and for precise alignment of the overlapping images, and chop-nod distances of $7''$–$9''$.

During our observations, we watched the data on a target accumulate over many chop/nod cycles. If there was no evidence of detection after about half an hour of wall clock time had been spent observing, we moved on to the next source. Tables 1 (Seyfert 1's) and 2 (Seyfert 2's) present the detections as well as data from the literature. For nondetections the 3 σ upper limits are set at the values of the faintest detection for each night, and these upper limits along with data from the literature are presented in Tables 3 and 4. We detected 31 Seyfert 1's and 31 Seyfert 2's spanning a wide range in flux (31 mJy to 26 Jy) and flux ratio ($\sim$9% to $\sim$100%) with respect to their *IRAS* fluxes (see Tables 1–4).

The observing conditions were diffraction-limited for 44 out of the 62 galaxies and were photometric or near photometric for all the observing nights. Standard stars from the Infrared Telescope Facility Bright Star Catalog and a 10.8 μm zero-magnitude flux of 33.4 Jy were used for calibration. Apertures of $1''.5$ (10 pixel) diameter were used for the photometry for both our standard stars and the AGNs so that flux from the first Airy ring would not be missed in the diffraction-limited cases and so that the full point-spread function would be sampled in the non–diffraction-limited cases. The errors quoted in Tables 1 and 2 are the statistical errors derived from the standard deviation of the magnitude zero points of standard stars throughout each night, the dominant source of our measurement errors. Following Maiolino et al. (1995) we apply no color correction in presenting our data in the tables.

The spectroscopic identifications of the sample are taken from the NASA Extragalactic Database (NED).[1] In presenting the results, we have chosen Seyfert 1's to include all Seyferts of types 1–1.5 and Seyfert 2's to include all Seyferts of types 1.8–2. It should be noted that the spectroscopic identifications in NED are not necessarily those used in the original sample of Rush et al. (1993).

The distances for this sample are determined on the basis of the redshifts from NED and with a Hubble constant of 70 km s^{-1} Mpc^{-1}. The sole exception is M81, where we have adopted a distance of 3.63 Mpc from Cepheid observations (Freedman et al. 1994).

4. STRUCTURE

The high resolution afforded by MIRLIN and the $0''.5$ beam on the 5 m telescope allow us to probe systematically for small-scale structure in AGNs and their host galaxies. Any extension more than two beams wide should have been easily detectable, setting our resolution limit at $1''$. The median value of the galaxies' distance is below 94 Mpc, which means that for half the galaxies we are probing on scales smaller than 460 pc.

All the detected sources, both Seyfert 1's and Seyfert 2's, show a point-source component (Fig. 1). Four Seyfert galaxies show a bright extended component along with the point source (Fig. 2). NGC 1068 shows an extension, first identified by Becklin et al. (1973), that extends north-northeast, consistent with previous mid-IR images by Tresch-Fienberg et al. (1987) and Bock et al. (2000). NGC 7469 is famous for its starburst ring, which was first identified as an extension in the mid-IR by Keto et al. (1992b) and then imaged by Miles, Houck, & Hayward (1994). After point-source subtraction, the NGC 7469 starburst ring becomes evident in the MIRLIN images. A southeastern extension in Arp 220 first seen by Keto et al. (1992a) is also present in the MIRLIN images. Mrk 1239 has a $\sim 1''$ extension to the northwest of its point source, which was previously unidentified in the mid-IR. It is similar to a blue extension (in $V-R$ color) in optical images from Mulchaey, Wilson, & Tsvetanov (1996).

For the rest of the sample we wished to make sure that the objects were in fact point sources; therefore, we scaled the standard stars at the same air mass as the Seyferts to the brightness of the AGN and then subtracted the two images from each other. If there was an obvious residual after point-source subtraction *and* the residual was the same from subtractions of two different standard-star observations, then we would regard the Seyfert as extended. None of the targets satisfied the two criteria. Thus, with the exception of the four objects above, all our targets are consistent with being point sources at the $1''$ level. A consequence of almost all the sources being unresolved is that *bright*, *compact* starbursts (such as NGC 7469 and Arp 220) or other *bright*, *compact* sources of emission (such as NGC 1068 and Mrk 1239) do not contribute to the nuclear 10 μm flux of Seyfert galaxies.[2]

[1] The NASA / IPAC Extragalactic Database is operated by the Jet Propulsion Laboratory, California Institute of Technology, under contract with the National Aeronautics and Space Administration.

[2] The closest galaxy imaged was M81 at 3.63 Mpc, where $1''$ corresponds to 18 pc, and we still detected only a point source using the above methodology. A more detailed study by Grossan et al. (2001) found evidence for very low level extended emission in this case.

TABLE 1

SEYFERT 1 DETECTIONS AND DATA FROM THE LITERATURE

Name	Type (from NED)	Distance[a] (Mpc)	Observation Date (UT)	M_N	N Band (This Paper)[b] (mJy)	N Band (Literature) (mJy)	Reference	Difference (mJy)	Ratio to *IRAS*[c]	Extended Flux Lower Limit[d](mJy)	$J-K_s$[e]
3C 120	Sy 1, S0	141	1999 Nov 25	−29.5	109 ± 35	220 ± 30	1	-109 ± 46	0.26	51	2.08
3C 234	Sy 1	791	2000 Mar 26	−33.3	110 ± 8	77 ± 7	2	33 ± 14	0.52	...	2.43
3C 273	Sy 1, blazar	678	2000 Mar 25	−33.8	247 ± 17	338 ± 14	3	-117 ± 22	0.32	...	1.77
3C 445	Sy 1	241	2000 Jul 12	−30.6	100 ± 10	...		...	0.20	...	2.20
IC 4329A	Sy 1.2, SA0	69	2000 Apr 13	−30.3	915 ± 48	770 ± 70	1	145 ± 85	0.91	...	2.12
IRAS 03450+0055	Sy 1	134	1999 Nov 26	−29.3	98 ± 13	170 ± 17	4	-72 ± 21	0.33	...	2.14
IRAS 07599+6508	Sy 1, QSO	637	1999 Nov 26	−33.3	180 ± 23	215 ± 11	4	-35 ± 25	0.57	...	2.66
IRAS 13349+2438	Sy 1	461	2000 Mar 26	−33.7	487 ± 34	...		...	0.76	...	2.32
IRAS 15091−2107	Sy 1	191	2000 Mar 26	−30.5	145 ± 11	...		...	0.59	...	1.88
I Zw A1	Sy 1, compact	262	1999 Nov 25	−32.0	298 ± 65	310 ± 30	1	-12 ± 72	0.73	...	2.31
M −5-13-17	Sy 1.5, S0/a	54	1999 Nov 27	−27.7	141 ± 16	...		...	0.71	...	1.21
M −6-30-15	Sy 1.2, E/S0	33	2000 Apr 13	−27.7	366 ± 19	286 ± 20	5	80 ± 28	1.3	...	1.80
Mrk 9	Sy 1, S0	171	1999 Nov 25	−29.3	58 ± 17	235 ± 24	4	-177 ± 29	0.27	63	2.10
Mrk 79	Sy 1.2, SBb	95	2000 Mar 25	−29.5	237 ± 16	255 ± 26	4	-18 ± 31	0.73	...	2.13
Mrk 231	Sy 1, SAc	181	2000 Apr 12	−32.7	1235 ± 60	1420 ± 360	1	-185 ± 365	3.0[f]	...	2.30
Mrk 335	Sy 1, S0/a	110	1999 Nov 25	−29.3	151 ± 33	210 ± 40	1	-59 ± 52	0.59	...	2.18
Mrk 509	Sy 1.2, compact	147	2000 Jul 12	−30.3	201 ± 14	240 ± 24	4	-39 ± 24	0.77	...	1.76
Mrk 704	Sy 1.5, SBa	125	2000 Mar 26	−30.4	297 ± 18	270 ± 27	4	27 ± 32	0.71	...	2.03
Mrk 817	Sy 1.5, SBc	135	2000 Apr 12	−30.2	234 ± 13	...		...	0.78	...	1.99
Mrk 1239	Sy 1.5, E/S0	85	2000 Mar 26	−29.5	286 ± 24	600 ± 60	4	-314 ± 65	0.39	173	2.40
NGC 931/Mrk 1040	Sy 1.5, Sbc	71	1999 Nov 26	−28.8	212 ± 28	333 ± 33	4	-121 ± 43	0.39	...	1.91
NGC 1194	Sy 1, SA0	57	1999 Nov 26	−27.8	133 ± 19	...		...	0.58	...	1.32
NGC 3227	Sy 1.5, SABpec	17	1999 Nov 27	−25.6	225 ± 24	280 ± 35	1	-55 ± 42	0.26	75	1.49
NGC 4051	Sy 1.5, SABbc	10	2000 Apr 12	−25.2	417 ± 22	260 ± 26	1	157 ± 34	0.32	...	1.63
NGC 4151	Sy 1.5, SABab	14	2000 Mar 25	−27.4	1520 ± 91	1400 ± 140	1	120 ± 17	0.91	169	1.87
NGC 4253/Mrk 766	Sy 1.5, SBa	55	2000 Mar 25	−28.4	253 ± 16	241 ± 28	4	12 ± 32	0.94	...	1.96
NGC 4593	Sy 1, SBb	39	2000 Mar 26	−27.6	257 ± 19	176 ± 18	4	81 ± 26	0.60	...	1.82
NGC 5548	Sy 1.5, SA0/a	74	2000 Mar 26	−29.2	292 ± 24	210 ± 20	1	82 ± 31	0.73	...	1.94
NGC 7469	Sy 1.2, SABa	70	1999 Nov 26	−29.1	310 ± 43	600 ± 60	1	-290 ± 74	0.25	330	1.69
NGC 7603	Sy 1.5, SAb	126	1999 Nov 25	−29.2	102 ± 39	77 ± 14	1	25 ± 41	0.20	...	1.90
UGC 5101	Sy 1	169	2000 Apr 12	−29.4	71 ± 8	107 ± 11	4	-36 ± 14	0.25	...	2.15

[a] Distance derived using $H_0 = 70$ km s^{-1} Mpc^{-1}.

[b] These fluxes are not color-corrected. Based on the spectral slopes from Edelson, Malkan, & Rieke 1987, the raw N-band fluxes must be multiplied by a factor of 1.24 to color-correct.

[c] The ratio to *IRAS* is taken with respect to the *IRAS* 10.8 μm value, which is derived from a power-law fit of the *IRAS* 12 and 25 μm values.

[d] The extended flux lower limit is the diffuse flux in a 1$''$.5 ring outside the 1$''$.5 diameter point-source photometry region of a point-source–subtracted image. It is not the total diffuse flux, since chopping and nodding automatically subtracts some of the host galaxy's flux.

[e] The near infrared J and K_s data are taken from the peak pixel value of each galaxy from 2MASS.

[f] The ratio is with respect to the *IRAS* 12 μm Sample value of 480 mJy in Rush et al. 1993, but the *IRAS* 12 μm value reported in Soifer et al. 1989 is 1930 mJy, which would make the ratio 0.8.

REFERENCES.—(1) Rieke 1978; (2) Elvis et al. 1984; (3) Sitko et al. 1982; (4) Maiolino et al. 1995; (5) Glass, Moorwood, & Eichendorf 1982.

TABLE 2

SEYFERT 2 DETECTIONS AND DATA FROM THE LITERATURE

Name	Type (from NED)	Distance[a] (Mpc)	Observation Date (UT)	M_N	N Band (This Paper)[b] (mJy)	N Band (Literature) (mJy)	Reference	Difference (mJy)	Ratio to *IRAS*[c]	Extended Flux Lower Limit[d] (mJy)	$J-K_s$[e]
Arp 220	Sy 2	78	2000 Apr 12	−28.5	142 ± 8	190 ± 30	1	−38 ± 31	0.36	80	1.95
CGCG 381-051	Sy 2, SBc	131	2000 Jul 12	−28.9	68 ± 8	...		...	0.090	...	1.31
IRAS 03362−1641	Sy 2, pec	158	1999 Nov 27	−30.1	148 ± 11	...		...	0.66	...	2.42
IRAS 04385−0828	Sy 2	65	1999 Nov 25	−28.3	161 ± 46	274 ± 27	2	−20 ± 53	0.33	...	2.01
IRAS 08572+3915	Sy 2	249	2000 Mar 26	−31.5	212 ± 15	260 ± 30	1	−49 ± 34	0.92	...	2.56
IRAS 15480−0344	Sy 2, S0	130	2000 Jul 12	−29.3	102 ± 10	...		...	0.51	38	1.40
IRAS 22017+0319	Sy 2	262	2000 Jul 12	−31.1	137 ± 10	...		...	0.69	...	2.30
M +0-29-23	Sy 2, SABb	107	2000 Apr 13	−28.2	58 ± 7	...		...	0.12	90	1.38
M −3-34-64	Sy 2, SBa	91	2000 Apr 12	−30.4	594 ± 30	...		...	0.76	...	1.14
M −3-58-7	Sy 2, SAB0/a	135	2000 Jul 12	−30.1	200 ± 15	...		...	1.0	...	1.93
Mrk 273	Sy 2	162	2000 Apr 12	−29.5	79 ± 11	98 ± 23	3	11 ± 25	0.56	36	1.83
Mrk 463 E	Sy 2	218	2000 Mar 26	−31.9	395 ± 30	...		...	1.0	...	3.37
Mrk 938	Sy 2, Sc	85	2000 Jul 12	−28.8	161 ± 12	241 ± 24	2	−70 ± 27	0.57	51	1.54
NGC 262/Mrk 348	Sy 2, SA0/a	64	1999 Nov 25	−27.9	117 ± 26	300 ± 30	3	−154 ± 40	0.26	...	1.88
NGC 1068	Sy 2, SAb	16	1999 Nov 26	−30.8	25588 ± 3200	18000 ± 1920	3	5150 ± 3800	0.72	13113	2.58
NGC 1320/Mrk 607	Sy 2, Sa	39	1999 Nov 26	−27.5	230 ± 27	28 ± 6	2	167 ± 28	0.97	...	1.38
NGC 2992	Sy 2, Sa pec	33	2000 Mar 26	−26.8	163 ± 13	196 ± 18	4	−11 ± 22	0.39	...	1.54
NGC 3031/M81	Sy 1.8, SAab	3	1999 Nov 26	−21.8	128 ± 16	86 ± 15	5	73 ± 22	0.020	...	1.17
NGC 4388	Sy 2, SAb	36	2000 Mar 25	−27.3	222 ± 15	404 ± 16	6	−159 ± 22	0.27	77	1.65
NGC 4579	Sy 1.9, SABb	22	2000 Mar 26	−25.1	77 ± 8	62 ± 16	6	18 ± 18	0.053	...	1.05
NGC 4922AB[f]	Sy 2, Sb	101	2000 Mar 26	−29.2	162 ± 12	115 ± 8	2	59 ± 14	0.70	...	1.69
NGC 4941	Sy 2, SABab	16	2000 Mar 26	−23.4	31 ± 5	...		...	0.080	...	1.10
NGC 4968	Sy 2, SAB0	42	2000 Mar 26	−27.8	250 ± 20	115 ± 10	2	165 ± 22	0.44	...	1.36
NGC 5135	Sy 2, SBab	59	2000 Apr 12	−27.7	119 ± 10	157 ± 20	2	−53 ± 22	0.27	283	1.38
NGC 5256	Sy 2, compact	119	2000 Mar 26	−28.7	72 ± 7	30 ± 5	2	37 ± 9	0.30	27	1.52
NGC 5347	Sy 2, SBab	33	2000 Mar 26	−27.1	213 ± 16	208 ± 9	2	18 ± 18	0.92	...	1.46
NGC 5506	Sy 1.9, Sa	26	2000 Mar 26	−28.1	835 ± 64	720 ± 72	2	196 ± 96	0.83	...	3.03
NGC 5995/M −2-40-4	Sy 2, S(B)c	108	2000 Mar 25	−29.7	224 ± 21	...		...	0.68	...	1.99
NGC 7172	Sy 2, Sa	37	2000 Jul 12	−26.6	107 ± 10	...		...	0.28	...	2.02
NGC 7314	Sy 1.9, SABbc	20	2000 Jul 12	−24.9	74 ± 8	...		...	0.14	...	1.79
NGC 7674	Sy 2, SAbc	125	1999 Nov 25	−30.2	254 ± 52	325 ± 33	2	−35 ± 62	0.47	...	2.18

[a] Distance derived using $H_0 = 70$ km s^{-1} Mpc^{-1}.

[b] These fluxes are not color-corrected. Based on the spectral slopes from Edelson et al. 1987, the raw N-band fluxes must be multiplied by a factor of 1.25 to color-correct.

[c] The ratio to *IRAS* is taken with respect to the *IRAS* 10.8 μm value, which is derived from a power-law fit of the *IRAS* 12 and 25 μm values.

[d] The extended flux lower limit is the diffuse flux in a 1″.5 ring outside the 1″.5 diameter point-source photometry region of a point-source–subtracted image. It is not the total diffuse flux since chopping and nodding automatically subtracts some of the host galaxy's flux.

[e] The near-infrared J and K_s data are taken from the peak pixel value of each galaxy from 2MASS.

[f] The *IRAS* value encompasses the 12 μm flux from NGC 4922A and NGC 4922B and so is labeled NGC 4922AB, which we have used here for cross-identification purposes. The 10 μm value quoted in the table is for NGC 4922B, which is identified in NED as a Seyfert 2 as well as a LINER and an H II region galaxy.

REFERENCES.—(1) Wynn-Williams & Becklin 1993; (2) Maiolino et al. 1995; (3) Rieke 1978; (4) Glass et al. 1982; (5) Rieke & Lebofsky 1978; (6) Scoville et al. 1983.

TABLE 3
SEYFERT 1 UPPER LIMITS AND DATA FROM THE LITERATURE

Name	Type (from NED)	Distance[a] (Mpc)	Observation Date (UT)	M_N	*N* Band (This Paper)[b] (mJy)	*N* Band (Literature) (mJy)	Reference	Ratio to *IRAS*[c]	$J-K_s$[d]
M −2-33-34.....	Sy 1, Sa	62	2000 Mar 26	>−26.4	<30	...		<0.12	1.38
Mrk 618	Sy 1, SBb pec	152	1999 Nov 25	>−29.0	<60	270 ± 27	1	<0.18	2.16
Mrk 1034	Sy 1, S?	144	1999 Nov 26	>−29.5	<100	79 ± 7	1	<0.32	1.43
NGC 1097.....	Sy 1, SBb	18	1999 Nov 25	>−24.4	<60	65 ± 9	2	<0.03	1.20
NGC 3511.....	Sy 1, SABc	15	2000 Mar 25	>−24.7	<110	6 ± 0.5	1	<0.03	1.10

[a] Distance derived using $H_0 = 70$ km s^{-1} Mpc^{-1}.
[b] These fluxes are not color-corrected. Based on the spectral slopes from Edelson et al. 1987, the raw *N*-band fluxes, and hence upper limits, must be multiplied by a factor of 1.24 to color-correct.
[c] The ratio to *IRAS* is taken with respect to the *IRAS* 10.8 μm value, which is derived from a power-law fit of the *IRAS* 12 and 25 μm values.
[d] The near-infrared *J* and K_s data are taken from the peak pixel value of each galaxy from 2MASS.
REFERENCES.—(1) Maiolino et al. 1995; (2) Telesco & Gatley 1981.

The question that follows is whether there was any *low-level, diffuse* emission detected for the rest of the sample. To answer this question, the flux within a 1.″5 wide ring outside the 1.″5 diameter central photometry region was measured on the point-source–subtracted images. If the flux contained within the ring was 3 σ greater than the noise, it is reported in Tables 1 and 2. Note that these values reflect the *difference* in flux between the ring and the nearby locations to which the telescope was chopping and nodding and that as such they reflect the *change* in diffuse emission near the centers of these Seyferts and not the total diffuse flux. The measurements are sensitive to the difference between the diffuse emission within ∼2.″5 of the nucleus and that outside of ∼4.″5 of the nucleus and so constitute a lower limit to the total diffuse flux. Four Seyfert 1's and six Seyfert 2's showed diffuse flux, having a median total flux over the annulus of ∼50% of the flux of the central point source for both Seyfert types. Combining these numbers with those AGNs that had bright extended emission yields six Seyfert 1's (19%) and eight Seyfert 2's (26%) with extended emission.

These numbers are too few to make statistically significant statements about diffuse emission trends for Seyfert galaxies at 10 μm, but we can compare them with results from other surveys. Krabbe et al. (2001) detected low-level, extended emission in four out of the eight Seyferts they imaged. One of the Seyferts with extended emission, NGC 1808, turned out to be a starburst galaxy, based on its X-ray to mid-IR correlation, leading to a final statistic of three out of seven or 43% with

TABLE 4
SEYFERT 2 UPPER LIMITS AND DATA FROM THE LITERATURE

Name	Type (from NED)	Distance[a] (Mpc)	Observation Date (UT)	M_N	*N* Band (This Paper)[b] (mJy)	*N* Band (Literature) (mJy)	Reference	Ratio to *IRAS*[c]	$J-K_s$[d]
ESO 541−IG 12.....	Sy 2, pec	242	1999 Nov 27	>−31.0	<140	...		<0.15	2.64
IRAS 05189−2524.....	Sy 2, pec	182	1999 Nov 24	>−30.4	<140	498 ± 50	1	<0.08	2.51
NGC 513.....	Sy 2, Sb/c	83	1999 Nov 26	>−28.3	<100	...		<0.35	1.33
NGC 1056.....	Sy 2, Sa	22	1999 Nov 26	>−25.4	<100	...		<0.22	1.27
NGC 1125.....	Sy 2, SAB0	46	1999 Nov 25	>−26.5	<60	...		<0.21	1.15
NGC 1241.....	Sy 2, SBb	57	1999 Nov 26	>−27.5	<100	79 ± 5	1	<0.26	1.15
NGC 1667.....	Sy 2, SABc	64	1999 Nov 26	>−27.8	<100	5 ± 2.5	1	<0.08	1.12
NGC 2639.....	Sy 1.9, SAa	47	1999 Nov 27	>−27.4	<140	8 ± 2.3	1	<0.15	1.00
NGC 3079.....	Sy 2, SBc	16	2000 Apr 12	>−24.3	<70	...		<0.02	2.02
NGC 3660.....	Sy 2, SBbc	52	2000 Mar 25	>−27.4	<110	33 ± 5	1	<0.07	1.16
NGC 3982.....	Sy 2, SABb	15	2000 Mar 25	>−24.8	<110	19 ± 6	1	<0.07	0.980
NGC 4501.....	Sy 2, SAb	32	2000 Mar 25	>−26.4	<110	6 ± 0.5	1	<0.01	1.15
NGC 4594.....	Sy 1.9, SAa	14	2000 Mar 26	>−23.2	<30	31 ± 9	1	<0.03	1.04
NGC 4602.....	Sy 1.9, SABbc	36	2000 Apr 13	>−25.9	<60	<53	1	<0.05	1.05
NGC 5005.....	Sy 2, SABbc	13	2000 Apr 12	>−24.0	<70	45 ± 7	1	<0.02	1.26
NGC 5033.....	Sy 1.9, SAc	12	2000 Apr 12	>−23.8	<70	24 ± 7	1	<0.03	1.26
NGC 5194/M51	Sy 2, SAbc	6	2000 Apr 12	>−22.2	<70	550 ± 250	2	<0.01	0.986
NGC 5929.....	Sy 2, Sab	35	2000 Mar 26	>−25.1	<30	24 ± 3	1	<0.09	1.38
NGC 5953.....	Sy 2, SAa	28	2000 Apr 13	>−25.4	<60	24 ± 7	1	<0.04	1.00
UGC 11680/Mrk 897.....	Sy 2, compact	112	2000 Apr 12	>−28.6	<70	60 ± 8	1	<0.11	1.13

[a] Distance derived using $H_0 = 70$ km s^{-1} Mpc^{-1}.
[b] These fluxes are not color-corrected. Based on the spectral slopes from Edelson et al. 1987, the raw *N*-band fluxes, and hence upper limits, must be multiplied by a factor of 1.25 to color-correct.
[c] The ratio to *IRAS* is taken with respect to the *IRAS* 10.8 μm value, which is derived from a power-law fit of the *IRAS* 12 and 25 μm values.
[d] The near-infrared *J* and K_s data are taken from the peak pixel value of each galaxy from 2MASS.
REFERENCES.—(1) Maiolino et al. 1995; (2) Kleinmann & Low 1970.

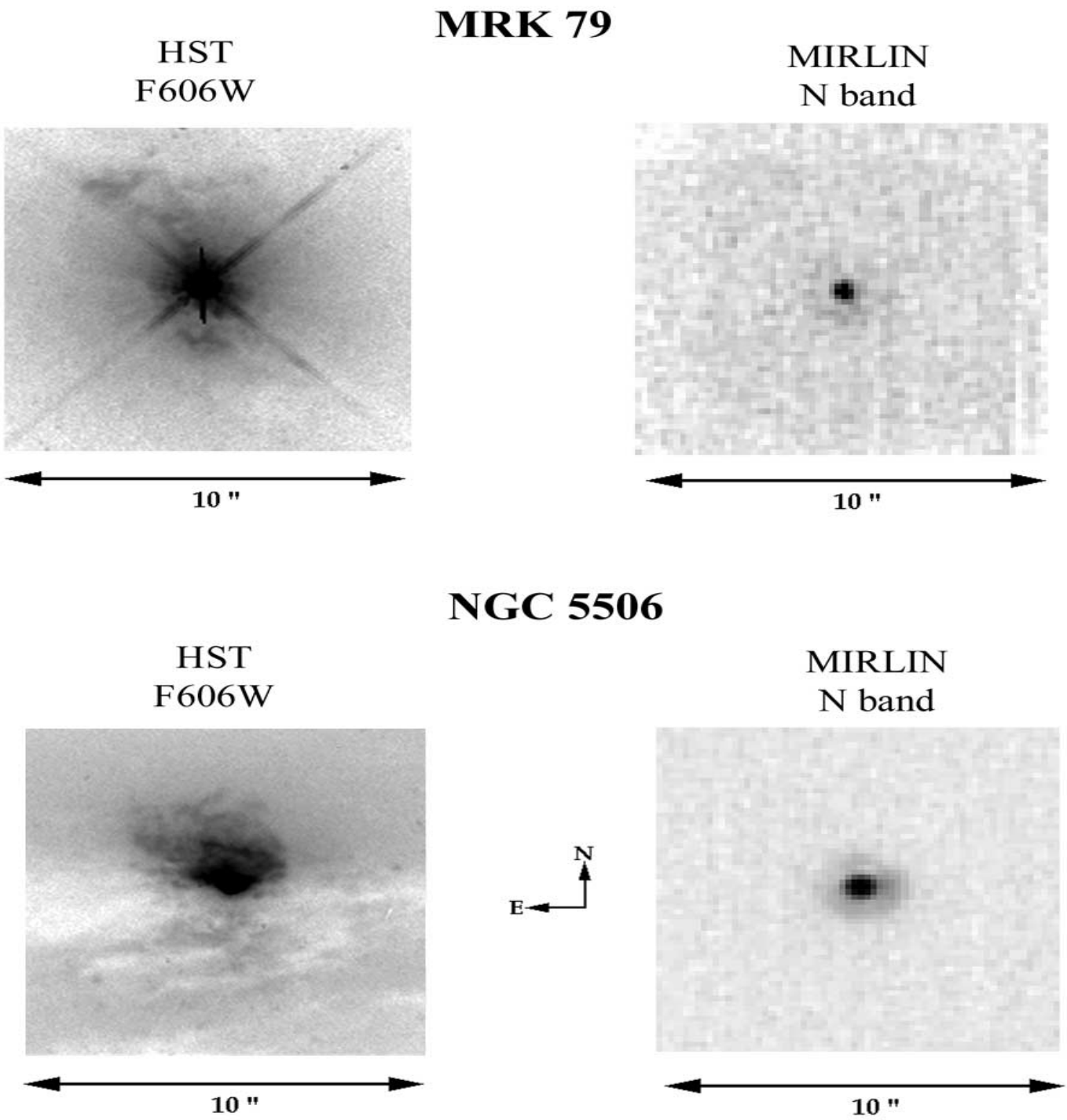

FIG. 1.—Top image is Mrk 79 showing a point source in the optical (note the diffraction spikes) and a point source in the mid-IR. The bottom image of NGC 5506 shows no point source in the optical, but a very bright one at *N*-band. Note the Airy ring around the 10 μm image showing that we are diffraction-limited. Both optical images are from Malkan et al. (1998).

extended emission. Although these are small-number statistics, there is a large difference between their extended emission detection rate and ours. Unfortunately, we do not have any targets in common to compare directly; still, we do not view these results as being in contradiction with the lower rate of extended emission detection in our sample, but more a reflection of the differences in our experiments. The on-chip chop/nod throw for MIRLIN was typically $7''$–$9''$, whereas Krabbe et al. (2001) had a chop/nod throw of $\sim 21''$. They thus subtracted less light from the host galaxy, leading to greater sensitivity to extended emission. Higher resolution imaging also resolves out diffuse emission, spreading it out over many more pixels with each pixel receiving much less flux, making it harder to detect.

This lower rate of diffuse emission detection can also be seen when compared with the large-beam *IRAS* fluxes (Tables 1–4). The smaller MIRLIN aperture can account for a significant part in the lower ratios, but the small chops/nods

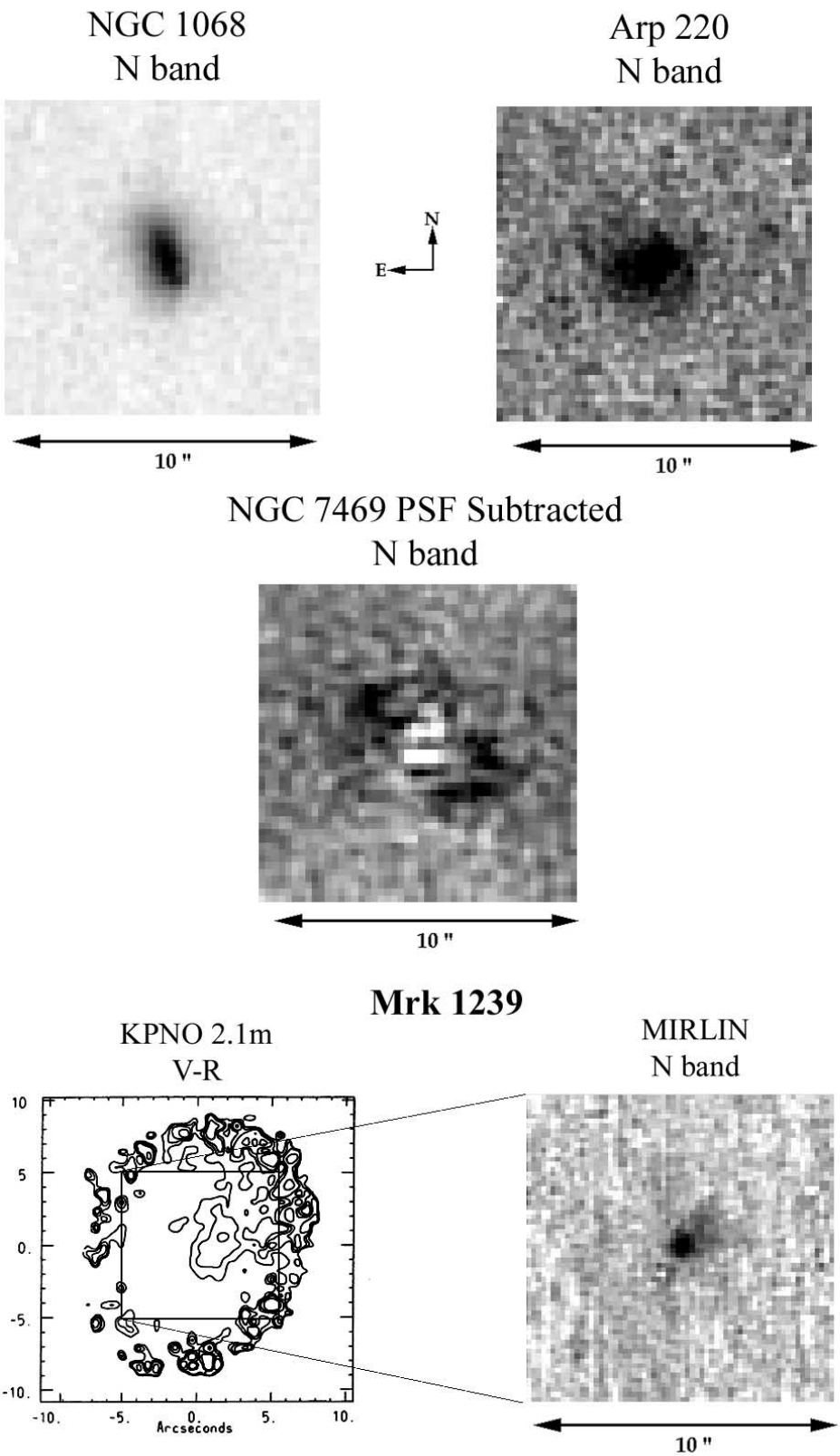

FIG. 2.—MIRLIN images of extended objects NGC 1068, Arp 220, NGC 7469 (point-source–subtracted), and Mrk 1239. For Mrk 1239 the *N*-band MIRLIN image is compared with an optical image by Mulchaey et al. (1996), with both showing an extension to the northwest [with $V-R = 1.35$; $\Delta(V-R) = -0.16$ (*outer contour*), -0.23, -0.3, and -0.37].

and the resolving out of diffuse emission due to higher resolution may mean that some flux within the apertures is missed.

Finally, although there has been a great deal of work on a starburst-AGN connection, it is not clear that the faint extended 10 μm emission detected in this survey necessarily comes from star formation. For example, the bright extended 10 μm emission for NGC 1068 comes from the dust-reprocessed optical/UV photons in its ionization cone (Bock et al. 2000), which may also be the case for Mrk 1239 since its ionization cone is aligned with its 10 μm emission. There is no reason to expect that the fainter emission around other Seyferts would be significantly different from the brighter emission, and it may be either from dust-reprocessed AGN continuum, from star formation, or from a combination of both.

5. PHOTOMETRIC COMPARISONS BETWEEN SEYFERT 1 AND SEYFERT 2 GALAXIES

We detected 31 out of 36 (86%) of the Seyfert 1's that we observed, but only 31 out of 51 (61%) of the Seyfert 2's that we observed. Selection effects must be taken into account before comparing these numbers. One very important selection effect is the distance distribution. Figure 3 shows the distances of detected objects versus Seyfert type. The Seyferts occupy the same range in distance except for four very luminous Seyfert 1's that have been detected at much greater distances than the rest of the sample.

Even without including the four outlying Seyfert 1's, the central point sources span more than 3 orders of magnitude in luminosity (M_N from -24.9 to -32.7). The *IRAS* 12 μm sample thus spans not only a wide range in total luminosity but also a wide range in central point source luminosity.

In spite of this, the absolute 10 μm luminosity distribution of the Seyfert 1's is quite comparable to that of the Seyfert 2's. The Seyfert 1 distribution has a median of -29.3 ± 0.3 without the four outliers (-29.4 ± 0.4 with the outliers), and the Seyfert 2 distribution has a median of -28.6 ± 0.4 (Fig. 4).

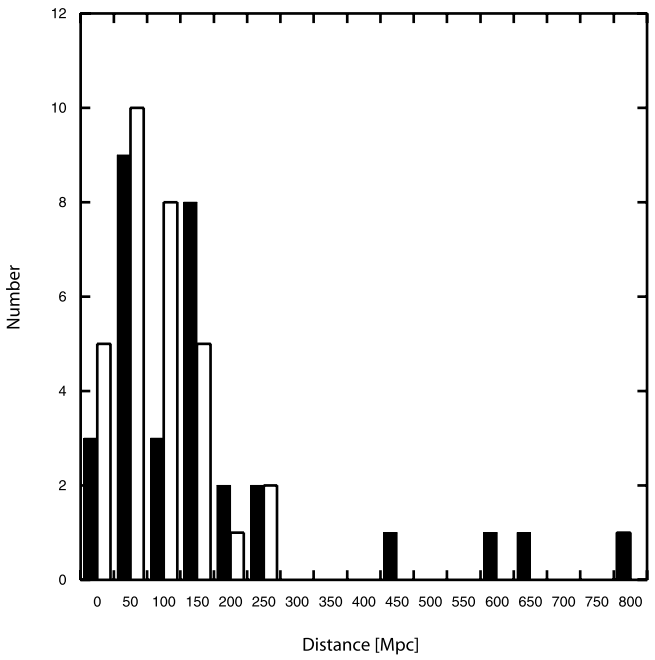

FIG. 3.—Distance histogram of detected Seyfert galaxies. Filled bars are Seyfert 1's and unfilled bars are Seyfert 2's.

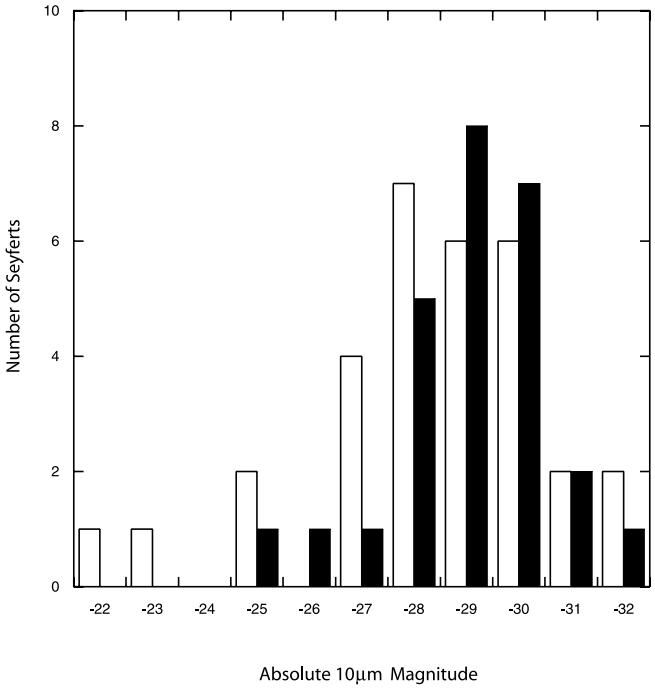

FIG. 4.—Luminosity distribution for detected Seyfert 1's and 2's, not including distant outliers. Filled bars are Seyfert 1's and unfilled bars are Seyfert 2's.

The apparent agreement of the luminosity distributions, however, disappears if we consider upper limits in addition to detections. Using the Kaplan-Meier[3] estimator to determine the median of a distribution containing upper limits, the median 10 μm luminosity of the expanded Seyfert 1 distribution changes little, from -29.3 ± 0.3 to -29.2 ± 0.4 (Fig. 5). In contrast, the median 10 μm luminosity of the Seyfert 2's changes by 1.3 mag (more than a factor of 3) from -28.6 ± 0.4 to -27.3 ± 0.5 (Fig. 6). The result is a Seyfert 2 median 1.9 ± 0.6 mag fainter than the Seyfert 1 median. Clearly, unless extinction is very great at 10 μm for the undetected objects, the Seyfert 2 luminosity distribution extends appreciably to lower limits.

6. VARIABILITY CANDIDATES

We have compared our small-aperture photometry to that from the literature ($\sim 5''$–$8''$ beams), and it has become evident that there are differences, which we interpret as possible variability at 10 μm. As a criterion for variability, we compare the difference between our data and the data from the literature, do a quadrature sum of the errors, and if the difference is 5 times greater than the quadrature sum of the errors, we consider a galaxy to be a candidate for variability.

There are two categories of variability: Seyferts that apparently became brighter in our sample, and Seyferts that apparently became dimmer. Since we are using a smaller aperture and are chopping and nodding on a small scale, we will lose some diffuse emission, as was pointed out in comparisons with Krabbe et al. (2001). The apparent decrease in flux may therefore simply be the result of comparing with

[3] The Kaplan-Meier values were determined using ASURV, rev 1.2 (LaValley, Isobe, & Feigelson 1992), which implements the methods presented in Feigelson & Nelson (1985).

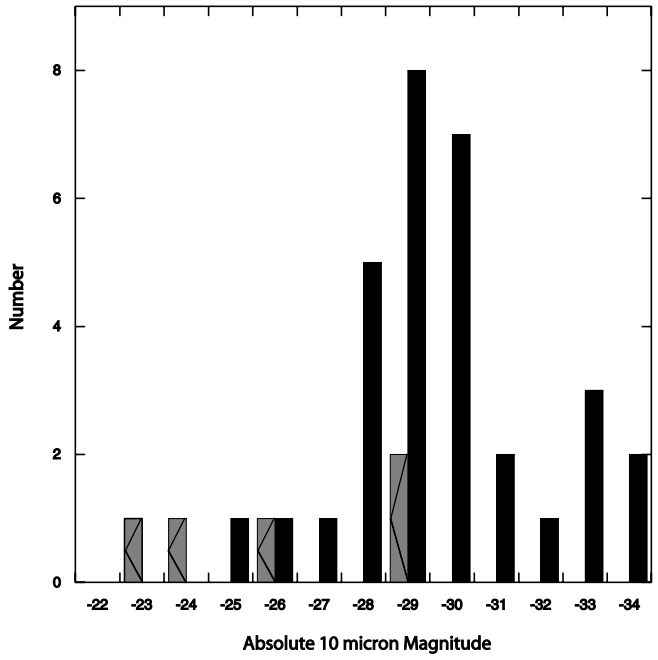

FIG. 5.—Luminosity distribution of Seyfert 1's. Filled bars are detections; shaded bars with arrows are upper limits.

larger aperture and larger chop/nod data. Thus, Seyferts that appear dimmer may not have varied at all, and we do not consider them as variability candidates.

Using the above criterion, one Seyfert 1 showed a significant increase in flux: NGC 4051. Although 10 μm variability has not been reported for this galaxy, Salvati et al. (1993) did detect a 2.2 μm flare in NGC 4051 in which the source brightened and dimmed by a factor of 2 in 6 months, so the 60% change at 10 μm may be a result of a similar flare.

Two Seyfert 2's increased their flux significantly: NGC 1320 and NGC 4968. NGC 1320 showed the greatest increase of any of the AGNs. Maiolino et al. (1995) reported a value of 28 ± 6 mJy for NGC 1320, while we detected 230 ± 27 mJy, an increase of a factor of 8. We repeated the observation 22 months later and measured a similar result: 210 ± 21 mJy. De Robertis & Osterbrock (1986) referred to NGC 1320 as a "feeble, high-ionization Seyfert 2 galaxy" on the basis of their optical spectroscopy, which showed a high ionization spectrum but very narrow lines and a weak, featureless continuum. Thus, both in the optical and in the infrared, this object is unique and merits continued monitoring. No infrared variability has been previously reported for NGC 4968; however, we measured an increase of 120% at 10 μm. Table 5 presents a summary of the above for all three variability candidates.

As stated above, we are not sensitive to decreases in flux. Still, it would seem reasonable to expect that as many Seyferts decreased in flux as increased, implying that perhaps six out of the 62 targets, or 10% of Seyferts, may be variable.

6.1. *Physical Interpretations of Variability*

Few data exist on 10 μm variability on long timescales for Seyfert galaxies. The closest comparison that can be made is with the two decade long multiwavelength monitoring campaign of 25 quasars by Neugebauer & Matthews (1999). They found a median variability of 13% at 10 μm in their sample of radio-quiet quasars, with the maximum variation being 28%. Hence, if the present three variability candidates are substantiated, they would provide the first demonstration of large-amplitude 10 μm variability in any radio-quiet AGN. The time span between our data and the data in the literature covers a range from 5 to 20 yr, so there is no canonical timescale to which we can assign the possible variations. However, the observed timescales can be used to see whether the variability is physically reasonable and, if we interpret the infrared variability as reverberation, to set limits on the bolometric luminosity of the illuminating source.

The timescale of thermal dust reverberation depends on the distance and distribution of the infrared-emitting dust around an optical/UV source as well as the luminosity of the source. A recent dusty torus model by Nenkova, Ivezić, & Elitzur (2002) successfully predicted many aspects of the IR emission from AGNs; the authors concluded that the majority of the 10 μm emission arose from the $\sim$500 K region of the torus, with the following relation between the radius of 500 K emission and the bolometric luminosity: $rL_{12}^{-1/2} = 10$ pc, where $L_{12} = L_{\rm bol}/10^{12}\ L_{\odot}$ is the illuminating bolometric luminosity.

Weedman (1976) showed that a typical Seyfert 1 nucleus has a bolometric luminosity that is 1000 times that of its broad Hβ luminosity. For NGC 4051 the Hβ flux is 4.3×10^{-13} ergs s^{-1} cm^{-2} (Nagao et al. 2000), corresponding to $L_{\rm bol} \sim 5 \times 10^{42}$ ergs s^{-1}. This luminosity would produce the majority of its 10 μm emission at a distance of 0.35 pc or 1.1 lt-yr, so the 22 yr time span between the 10 μm observations does little to set any limits on NGC 4051.

Unlike Seyfert 1's, Seyfert 2's do not have an easy method for predicting their bolometric luminosity. The above formula can, however, be used to set limits on the illuminating luminosity if reverberation is the source of the variability. For NGC 1320 the timespan for its variability is 5 yr, meaning that the dust would have to be at most 5 lt-yr away from the illuminating source; hence, $L_{\rm bol} < 1.2 \times 10^{44}$ ergs s^{-1}. For NGC 4968 the timespan is 6 yr, resulting in $L_{\rm bol} < 1.6 \times 10^{44}$ ergs s^{-1}.

Another possible source of 10 μm emission and hence 10 μm variability is nonthermal synchrotron radiation. Since

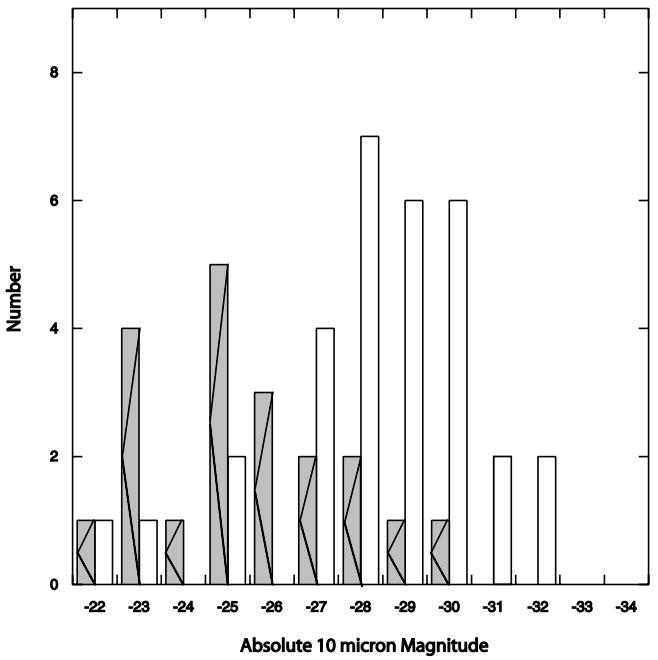

FIG. 6.—Luminosity distribution of Seyfert 2's. Open bars are detections; shaded bars with arrows are upper limits.

TABLE 5
SEYFERT 1 AND 2 VARIABILITY CANDIDATES

Name	Type (from NED)	Observation Date (UT)	N Band (This Paper) (mJy)	N Band (Literature) (mJy)	Reference	Percent Increase
NGC 4051	Sy 1.5	2000 Apr 12	417 ± 22	260 ± 26	1	60
NGC 1320/Mrk 607	Sy 2	1999 Nov 26	230 ± 27	28 ± 6	2	720
	...	2001 Sep 29	210 ± 21	...		...
NGC 4968	Sy 2	2000 Mar 26	250 ± 20	115 ± 10	2	120

REFERENCES.—(1) Rieke 1978; (2) Maiolino et al. 1995.

nonthermal radiation originates on small scales, its variability timescale can be as small as days. It is thus not limited in any way by the detected 5 yr span and may in fact provide a mechanism for the variability observed in all the above sources. The difficulty with this interpretation is that AGNs that have IR emission dominated by synchrotron radiation are radio-loud, while the three AGNs in question are considered to be radio-quiet (Rush, Malkan, & Edelson 1996).

7. BULGE COLOR VERSUS 10 μm MAGNITUDE DIAGRAM

From the extensive work done on normal galaxies using the Two Micron All Sky Survey (2MASS), it has been shown that regardless of galaxy type, spiral or elliptical, the predominant $J-K_s$ bulge color has a value of 1 with little scatter, while the host galaxies of AGNs tend to have redder central bulge colors (Jarrett 2000; Jarrett et al. 2003) because of the contribution of the AGNs. To explore how the near-IR properties of the centers of AGN host galaxies correlate with their 10 μm properties and to better characterize the role of host-galaxy dust extinction in the 10 μm flux, we have plotted the $J-K_s$ colors of the central pixels of the host galaxies versus the absolute N-band magnitudes obtained in this survey.[4]

A plot of central-pixel $J-K_s$ versus the absolute N magnitude in Figure 7 for objects closer than 300 Mpc shows a trend of redder $J-K_s$ colors, corresponding to more luminous N magnitudes. Alonso-Herrero et al. (2001) conducted deconvolutions of the bulge and nuclear contributions of a sample of Seyfert galaxies and showed that the J contribution of the nonstellar nucleus was small. The implication of that result in combination with the color-magnitude diagram is that the N-band luminosity is correlated with the K_s-band luminosity for the AGN component. The more the hot dust contributes to the central pixel in the 2MASS data, the redder the color becomes, and the stronger the N-band signal. The least 10 μm–luminous objects, represented by the upper limits, have predominantly bulge-like nuclear colors. These trends are followed by both Seyfert 1's and Seyfert 2's.

The host-galaxy extinction becomes evident for the objects that do not follow the trend of redder $J-K_s$ with more luminous N and are displaced in the direction of the reddening vector. In these cases the bulge is reddened by intervening dust, whether due to high inclination or to merging. Three such objects are Mrk 463 E, NGC 3079, and NGC 5506, all of which are significantly displaced from the rest of the Seyferts. Mrk 463 E is a well-known interacting galaxy (i.e., Mazzarella & Boroson 1993), while NGC 3079 and NGC 5506 are both edge-on spirals. A few objects are displaced to a lesser extent from the rest of the Seyferts and likely have some host-galaxy extinction affecting their K_s flux.

A second type of outlier is M −3-34-64, which has a normal central bulge color but seemingly excess 10 μm emission relative to other Seyferts in the sample. The cause of the position of this object may in fact be a lack of K_s-band emission due to circumnuclear extinction. Since dust extinction is less at N than at K ($A_N/A_V \sim 0.06$ vs. $A_K/A_V \sim 0.13$; Mathis 1990), there may be situations where sufficient extinction can eliminate K_s light from the Seyfert nucleus but allow N-band light to pass. The central $J-K_s$ bulge colors will not then be made redder by the addition of K_s light from the Seyfert nucleus, but enough 10 μm radiation will still escape to displace the AGN from others in the sample. For M −3-34-64 to be in the middle of the trend followed by the other AGNs, it would need to be at least 2 mag redder in $J-K_s$ color. Using the above extinction laws, this translates into an A_V of ~15, which would shift the AGN by only 1 mag at N.

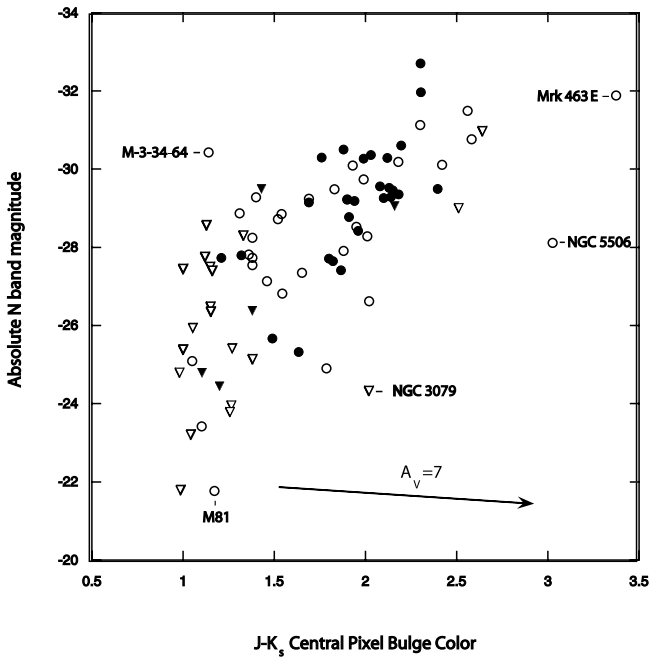

FIG. 7.—$J-K_s$ vs. absolute N magnitude for 2MASS central pixel flux, not including distant outliers. Filled circles are Seyfert 1's and unfilled circles are Seyfert 2's. Filled triangles are Seyfert 1 upper limits and unfilled triangles are Seyfert 2 upper limits. The extinction law is from Mathis (1990).

[4] The final 2MASS Atlas image is constructed from multiple subpixel dithered images, which are obtained with 2″.5 beams at J, H, and K_s. The separate images are mosaicked together into a final image that has a scale of 1″ pixel^{-1}. The host-galaxy central pixel is determined by centroiding over the combined J, H, and K_s mosaicked images. This pixel, which is also the brightest pixel except in galaxies that have heavy dust extinction, is the pixel most dominated by emission from the active nucleus.

In any case, all of the above outliers are Seyfert 2's, consistent with the view that extinction is the cause of the difference between Seyfert 1's and 2's and that we have a less extinguished view of the AGNs in Seyfert 1's than in Seyfert 2's.

8. COMPARISON WITH THE UNIFIED MODEL

The basic unified model uses a dusty torus to obscure the view of the accretion disk based on the angle of the observer. In this context, the infrared light that we see comes not from the accretion disk but from light absorbed and reradiated by dust in the torus. Some debate remains about whether all the IR light is thermal, and the variable Seyferts noted above may be the result of a combination of thermal and nonthermal components, but for the purposes of this comparison we will assume that all light from 1 to 10 μm comes from differing dust temperature regions in the torus.

8.1. *Morphology and Photometry*

Our most direct result is that both Seyfert 1's and Seyfert 2's show unresolved point sources in all their 10 μm images. This has already been noted for smaller samples of AGNs imaged at 10 μm (Soifer et al. 2000; Krabbe et al. 2001). Half our sample is probed on size scales smaller than 460 pc. The unified model predicts no significant differences at these size scales for Seyfert 1's and 2's. Thus our data put an upper limit on the size of the 10 μm emitting region and are consistent with the unified model.

Seyfert 1's and Seyfert 2's do not universally show point sources at shorter wavelengths, as demonstrated by two *HST* studies. Malkan, Gorjian, & Tam (1998), in their optical study of Seyferts, found that only 70% of the Seyfert 1's and none of the Seyfert 2's in their sample showed point sources. Quillen et al. (2001), in their near-IR (1.2–2.2 μm) *HST* study, found that all their Seyfert 1's but only 50% of their Seyfert 2's showed point sources.

The growing presence of point sources for both Seyfert 1's and 2's at longer wavelengths fits well with the dusty torus model. In the optical, dust from the torus blocks all light from the accretion disk, so none of the Seyfert 2's show point sources. While the torus should not block the disk of a Seyfert 1, dust in the host galaxy may still do so, resulting in only 70% of the Seyfert 1's showing point sources. Dust in the host galaxy is not an actual part of the unified model but cannot be discounted (Malkan et al. 1998; Schmitt et al. 2001).

At near-IR, all the Seyfert 1's show point sources, since the tori are not blocking and near-IR light can effectively penetrate most dust obscuration from the host galaxy. Seyfert 2's still show point sources only 50% of the time since in some cases the tori are thick enough to block the near-IR emitting region. The amount of dust through which we are looking is a function of the viewing angle, and the 50% of point sources that we do not detect may include ones that we are looking at close to edge-on. In extreme cases (e.g., NGC 5506), dust in the host galaxy may also contribute to the hiding of the point source in the near-IR.

At 10 μm, all detected Seyferts show point sources, indicating that the 10 μm emitting region is relatively easily accessible, regardless of torus orientation and host-galaxy obscuration. This lack of obscuration is also evident in the luminosity distribution of the Seyfert 1's and 2's (Fig. 4), where there are Seyfert 2's that are as luminous as the Seyfert 1's. The similarity at the more luminous end indicates that the Seyfert 2 luminosity distribution is not simply an extinguished version of the Seyfert 1 distribution. This does not contradict the unified model, but adds the requirement that torus models must produce Seyfert 1's and 2's that can have similarly high 10 μm luminosities.

One question remains concerning the low-luminosity, nondetected Seyfert 2's: are they merely faint, or are they very heavily obscured? For extinction to be the cause of the nondetection, an extremely large amount of dust would be required. To shift a Seyfert 2 in the luminosity distribution from the median to the low-luminosity tail would require $A_N = 7$ (Fig. 6), which would translate into $A_V = 120$. These objects are candidates for X-ray follow-up to see if the X-ray–derived extinction matches the $A_V = 120$ postulated by the 10 μm luminosity shift. If the nondetections turn out to be simply underluminous Seyfert 2's, then the unified model would have to be modified to distinguish between obscured Seyfert 2's and low-luminosity Seyfert 2's and to explain why there are few low-luminosity Seyfert 1's.

8.2. *Color-Magnitude Relation*

A feature in the $J-K_s$ versus N diagram may provide more direct support for the dusty torus model. The Seyfert 2 M−3-34-64, which shows bulge-like $J-K_s$ colors but has 10 μm luminosity greater than other AGNs in the sample with these colors, may in fact be a case where the torus is being viewed edge-on. In this case the torus may be thick enough to absorb all of the J and K_s light, preventing the Seyfert nucleus from affecting the central bulge color of the host galaxy, but still thin enough to allow the more dust-penetrating N-band light to escape.

9. SUMMARY AND CONCLUSIONS

1. We observed 87 galaxies at N band from the Extended 12 μm Sample and detected 62: 31 Seyfert 1's and 31 Seyfert 2's. The detection rate for Seyfert 1's was 86%, while the rate for Seyfert 2's was 61%.

2. The fluxes of the detected Seyferts span a factor of 400, while the luminosities span a factor of 4000.

3. The trend of increasing point-source domination from the optical to the near-IR continues out to 10 μm, where all the detected Seyferts show a bright point-source component. Fifty-eight out of the 62 galaxies are consistent with being point sources down to a resolution of 1″, which for the median distance of 94 Mpc translates to a distance of 460 pc. The remaining four have bright extended emission surrounding a point source.

4. Of the four AGNs that showed bright extended emission, Arp 220, NGC 1068, NGC 7469, and Mrk 1239, only Mrk 1239's extended emission was previously undetected.

5. Faint extended emission is detected in the nuclei of four Seyfert 1's and six Seyfert 2's. When combined with the bright extended emission numbers, this yields a total of six Seyfert 1's (19%) and eight Seyfert 2's (26%) with detected extended emission.

6. The detected Seyfert 1's and Seyfert 2's have similar luminosity distributions, but the greater number of upper limits for Seyfert 2's shows that the Seyfert 2 luminosity distribution extends to less luminous values either intrinsically or because of greater extinction.

7. In a comparison of $J-K_s$ central bulge color with absolute N magnitude, luminous N magnitudes correspond to redder $J-K_s$ colors. One set of outliers from this trend is likely caused by host-galaxy extinction, since the shifts are in the direction of the reddening vector. Another individual outlier may be the

result of an edge-on torus absorbing *J*- and K_s-band light while allowing *N*-band light to escape. This color-magnitude relation can be a useful tool in identifying AGNs whose host galaxies are absorbing some of their IR emission.

8. Over timescales of 5–20 yr, one Seyfert 1 and two Seyfert 2's show a rise in their 10 μm flux, suggesting that they are variable. By symmetry, it would seem likely that as many of the Seyfert 1's and 2's also decreased in flux. This would mean that $\sim$10% of these objects are variable at 10 μm.

V. G. acknowledges support from the National Research Council. We thank G. Rieke and M. Malkan for helpful discussions and the Palomar staff for their aid in obtaining the data. We thank L. Rebull for her aid and the anonymous referee for helpful comments. Development of MIRLIN was supported by the JPL Director's Discretionary Fund, and its continued operation is funded by a supporting Research and Technology award from NASA's Office of Space Science. This publication makes use of data products from the Two Micron All Sky Survey, which is a joint project of the University of Massachusetts and the Infrared Processing and Analysis Center, funded by the National Aeronautics and Space Administration and the National Science Foundation. The research described in this paper was carried out by the Jet Propulsion Laboratory, California Institute of Technology, under contract to the National Aeronautics and Space Administration. Observations at the Palomar Observatory were made as a part of a continuing collaborative agreement between Palomar Observatory and JPL.

REFERENCES

Alonso-Herrero, A., Quillen, A. C., Simpson, C., Efstathiou, A., & Ward, M. J. 2001, AJ, 121, 1369
Antonucci, R. 1993, ARA&A, 31, 473
Becklin, E. E., Matthews, K., Neugebauer, G., & Wynn-Williams, C. G. 1973, ApJ, 186, L69
Bock, J. J., et al. 2000, AJ, 120, 2904
de Robertis, M. M., & Osterbrock, D. E. 1986, ApJ, 301, 98
Edelson, R. A., Malkan, M. A., & Rieke, G. H. 1987, ApJ, 321, 233
Elvis, M., Willner, S. P., Fabbiano, G., Carleton, N. P., Lawrence, A., & Ward, M. 1984, ApJ, 280, 574
Feigelson, E. D., & Nelson, P. I. 1985, ApJ, 293, 192
Freedman, W. L., et al. 1994, ApJ, 427, 628
Giuricin, G., Mardirossian, F., & Mezzetti, M. 1995, ApJ, 446, 550
Glass, I. S., Moorwood, A. F. M., & Eichendorf, W. 1982, A&A, 107, 276
Grossan, B., Gorjian, V., Werner, M. W., & Ressler, M. E. 2001, ApJ, 563, 687
Jarrett, T. H. 2000, PASP, 112, 1008
Jarrett, T. H., Chester, T., Cutri, R., Schneider, S. E., & Huchra, J. P. 2003, AJ, 125, 525
Keto, E., Ball, R., Arens, J., Jernigan, G., & Meixner, M. 1992a, ApJ, 387, L17
———. 1992b, ApJ, 389, 223
Kleinmann, D. E., & Low, F. J. 1970, ApJ, 161, L203
Krabbe, A., Böker, T., & Maiolino, R. 2001, ApJ, 557, 626
LaValley, M., Isobe, T., & Feigelson, E. D. 1992, BAAS, 24, 839
Maiolino, R., Ruiz, M., Rieke, G. H., & Keller, L. D. 1995, ApJ, 446, 561
Malkan, M. A., Gorjian, V., & Tam, R. 1998, ApJS, 117, 25
Mathis, J. S. 1990, ARA&A, 28, 37
Mazzarella, J. M., & Boroson, T. A. 1993, ApJS, 85, 27
Miles, J. W., Houck, J. R., & Hayward, T. L. 1994, ApJ, 425, L37
Mulchaey, J. S., Wilson, A. S., & Tsvetanov, Z. 1996, ApJS, 102, 309
Nagao, T., Murayama, T., Taniguchi, Y., & Yoshida, M. 2000, AJ, 119, 620
Nenkova, M., Ivezić, Ž., & Elitzur, M. 2002, ApJ, 570, L9
Neugebauer, G., & Matthews, K. 1999, AJ, 118, 35
Peterson, B. M., ed. 1997, An Introduction to Active Galactic Nuclei (Cambridge: Cambridge Univ. Press)
Quillen, A. C., McDonald, C., Alonso-Herrero, A., Lee, A., Shaked, S., Rieke, M. J., & Rieke, G. H. 2001, ApJ, 547, 129
Ressler, M. E., Werner, M. W., Van Cleve, J., & Chou, H. A. 1994, Exp. Astron., 3, 277
Rieke, G. H. 1978, ApJ, 226, 550
Rieke, G. H., & Lebofsky, M. J. 1978, ApJ, 220, L37
Rush, B., Malkan, M. A., & Edelson, R. A. 1996, ApJ, 473, 130
Rush, B., Malkan, M. A., & Spinoglio, L. 1993, ApJS, 89, 1
Salvati, M., et al. 1993, A&A, 274, 174
Schmitt, H. R., Antonucci, R. R. J., Ulvestad, J. S., Kinney, A. L., Clarke, C. J., & Pringle, J. E. 2001, ApJ, 555, 663
Scoville, N. Z., Becklin, E. E., Young, J. S., & Capps, R. W. 1983, ApJ, 271, 512
Sitko, M. L., Stein, W. A., Zhang, Y.-X., & Wisniewski, W. Z. 1982, ApJ, 259, 486
Soifer, B. T., Boehmer, L., Neugebauer, G., & Sanders, D. B. 1989, AJ, 98, 766
Soifer, B. T., et al. 2000, AJ, 119, 509
Telesco, C. M., & Gatley, I. 1981, ApJ, 247, L11
Tresch-Fienberg, R., Fazio, G. G., Gezari, D. Y., Lamb, G. M., Shu, P. K., Hoffmann, W. F., & McCreight, C. R. 1987, ApJ, 312, 542
Weedman, D. W. 1976, ApJ, 208, 30
Wynn-Williams, C. G., & Becklin, E. E. 1993, ApJ, 412, 535